STU
SLOVAK UNIVERSITY OF TECHNOLOGY IN BRATISLAVA

Journal of Electrical Engineering, Vol. 77, No. 1, 2026, pp. 41-54
https://reference-global.com/journal/JEE

Multiresolution analysis for estimating switching transient overvoltages in transmission lines

Predrag Petrović, Dimitrije Rozgić

Energization of an unloaded transmission line produces switching transient overvoltages, the magnitude and shape of which are highly dependent on the point-on-wave at which the switching operation is initiated. These transients can impose dielectric stress on insulation and associated equipment in some circumstances – depending on the transient amplitude, spectral content and location – and therefore may affect system reliability. Accurate estimation of their magnitude is therefore essential for effective insulation coordination, transient suppression, and protection system design. This paper presents a multiresolution analysis-based algorithm for accurately estimating the magnitude of switching transient overvoltages during transmission line energization. New analytical expressions are derived for the efficient extraction and characterization of transient components, providing improved accuracy and computational efficiency compared to conventional methods. The proposed method decomposes the recorded transient waveform into approximation and detail components using the Haar wavelet and its associated scaling function. The Haar wavelet is selected for its orthogonality, compact support, and computational efficiency, enabling rapid and precise time-frequency localization of transient phenomena. By isolating the high-frequency components associated with switching events, the algorithm provides an accurate estimation of the peak overvoltage magnitude. Simulation results verify the effectiveness of the proposed MRA-based approach in accurately estimating transient overvoltages with reduced computational burden compared to conventional time-domain and frequency-domain methods. The findings confirm that the technique provides a robust and efficient framework for the analysis and quantification of switching transients in high-voltage transmission systems, thereby enhancing system protection and insulation design.

Keywords: Haar wavelet, insulation coordination, multiresolution analysis (MRA), power system transient, switching transient, transmission line energization

1 Introduction

Switching overvoltages generated during the energization of high-voltage transmission lines represent a significant challenge for modern power systems. When a transmission line is connected to the network or re-energized after an outage, transient phenomena such as trapped charge, resonance, traveling waves, and high-frequency oscillations may lead to peak voltages significantly above steady-state levels. These overvoltages have important implications for insulation coordination, equipment aging, and overall system reliability [1-3]. Proper modeling of the line and its transient behavior is essential. Guidelines for switching transient analysis emphasize the need for distributed-parameter, multi-phase models, and, where necessary, frequency-dependent parameters in the ground propagation mode [1]. However, classical modeling and time-domain simulation techniques alone may not fully capture the wideband, high-frequency content of the transient signal – particularly the fast front components, reflections, and distortion effects inherent to energization and fault scenarios. This motivates the use of advanced signal processing methods for accurate transient overvoltage estimation.

In recent years, signal processing techniques based on wavelets and multiresolution analysis (MRA) have gained popularity for transient analysis in power systems. MRA decomposes a non-stationary signal into approximation (low-frequency) and detail (high-frequency) components at multiple scales, offering both time and frequency localization [4, 5]. In the context of transmission lines, MRA has been successfully applied to fault detection, classification, and location by analyzing high-frequency detail coefficients of current or voltage signals [4]. For instance, [1] proposes time-frequency multiresolution of high-frequency signals using mathematical morphology and spectral energy indices.

Several computational tools are also available for studying switching transient overvoltages while accounting for relevant system parameters [6]. However, some critical parameters are often unavailable or neglected in certain network configurations. One such parameter is a prestrike during circuit breaker closing, which refers to the formation of an electrical arc between fixed and moving contacts prior to contact closure [7]. Consequently, surge parameters predicted by analytical models or numerical simulation models may deviate

Faculty of Technical Sciences Čačak, University of Kragujevac, Čačak, 32000 Serbia
predrag.petrovic@ftn.kg.ac.rs, dinmitrije.rozgic@ftn.kg.ac.rs

https://doi.org/10.2478/jee-2026-0005, Print (till 2015) ISSN 1335-3632, On-line ISSN 1339-309X

from actual values, and precise determination often necessitates experimental measurements. Prestrike significantly affects transient overvoltage characteristics, including magnitude, waveform shape, and frequency, resulting in deviations between analytical or simulation predictions and actual measurements. While the Fourier transform is well recognized for its suitability in analyzing stationary phenomena, the wavelet transform provides superior time-frequency localization, making it particularly effective for the detailed analysis of dynamic transient events [8].

Despite advances in simulation and measurement techniques, there is a relative paucity of studies specifically targeting the estimation of switching transient overvoltage magnitudes during transmission line energization using MRA. Unlike conventional spectral methods, MRA allows accurate discrimination between overlapping transient phenomena and the background steady-state waveform [4, 9]. Its multiscale filtering structure can isolate fast electromagnetic traveling waves from slower resonant or electromechanical components, while naturally suppressing high-frequency noise [10, 11]. Consequently, MRA has been successfully applied in transient detection, fault location, and insulation coordination analyses where rapid response is required [12]. Furthermore, MRA-based features have been successfully combined with machine learning approaches for transient event classification and overvoltage magnitude estimation, enhancing predictive monitoring and system protection [1, 4].

In this paper, we propose a methodology to estimate the magnitude of switching transient overvoltages during transmission line energization by applying multiresolution analysis to measured or simulated voltage waveforms. The approach involves:

1. Extracting multi-scale detail coefficients from the voltage signal using discrete wavelet transform (DWT).
2. Correlating selected detail-level energies with the peak overvoltage amplitudes.
3. Providing a rapid and computationally efficient estimation tool suitable for complementing detailed EMT simulations and supporting system planning and operational decisions.

The proposed methodology offers the following novelties and contributions:

- Application of MRA specifically for peak overvoltage estimation in transmission line energization scenarios.
- Demonstration of the effectiveness of detail-level coefficients as predictors of transient overvoltage magnitude.
- A framework compatible with both measured and simulated waveforms, enabling practical deployment for system monitoring and planning.

2 Multiresolution analyses

When a transmission line is energized, the voltage at the breaker terminal exhibits a slow-front transient composed of travelling waves, reflections, and resonance phenomena, consistent with IEC/IEEE classifications [13]. Although categorized as a slow-front event, localized arc phenomena during breaker pre-strike or arc reignition may introduce short-duration high-frequency components, resulting in steep voltage variations embedded within the overall transient waveform.

To analyze these effects, the measured or simulated voltage signal $v(t)$is decomposed using multiresolution analysis (MRA) into approximation and detail components across successive resolution levels. The decomposition is expressed as

$$v(t) = A_J(t) + \sum_{j=1}^{J} D_j\,(t) \tag{1}$$

where $A_J(t)$ represents the low-frequency envelope and $D_j(t)$ captures transient components at scale j. The detail coefficients obtained from the discrete wavelet transform (DWT) provide direct information about the timing and energy of fast transient events.

By appropriate selection of the mother wavelet, MRA can be tuned to match the steep-front and oscillatory characteristics of switching surges. For typical sampling frequencies used in transient studies, detail levels corresponding to the 10 to 300 kHz range capture the dominant energy of transmission-line energization events.

The estimation of the peak switching overvoltage $V_{\max}$ is based on quantitative features extracted from the wavelet coefficients. A commonly used indicator is the detail-level energy

$$E_j = \sum_n |\, D_j(n)\,|^2 \tag{2}$$

which represents the transient energy content at scale j. In addition, the maximum absolute value of the detail coefficients provides a direct measure correlated with the instantaneous voltage rise. These features form the basis for estimating $V_{\max}$ without requiring exhaustive electromagnetic transient simulations.

Empirical studies have shown that high-frequency detail levels exhibit strong correlation with peak overvoltages obtained from EMT simulations, enabling rapid estimation with low computational cost. Owing to the fast pyramid algorithm of the DWT and the compact support of Haar wavelets, the approach is well suited for real-time implementation [14]. While estimation accuracy depends on wavelet selection, decomposition depth, and sampling frequency, Haar wavelets offer a favorable trade-off between simplicity, speed, and robustness.

In the proposed approach, MRA is formulated using a sequence of nested approximation spaces V_j, satisfying $V_j \subset V_{j+1}, V_{j+1} = V_j \oplus W_j$, where W_j denotes the wavelet space capturing details lost at level j (see Fig. 1) [15]. The approximation spaces represent low-frequency components, while the wavelet spaces isolate high-frequency transient features.

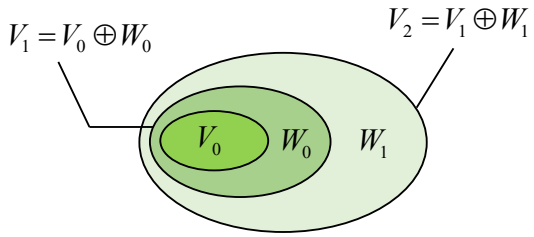

Fig. 1. Approximation and wavelet spaces

The approximation space V_j consists of functions of the form $\sum_{k\in Z} a_k \phi(2^j t - k), a_k \in R, j \in N$, where $\phi(t)$ is the scaling function. The wavelet space W_j is generated from scaled and translated versions of the mother wavelet $\psi(t)$

$$\sum_{k\in\mathbb{Z}} a_k \ \psi(2^j t - k), a_k \in \mathbb{R}. \tag{3}$$

Any square-integrable signal $f(t) \in L^2(\mathbb{R})$ can therefore be represented as [15]

$$f(t) = \sum_k s_{J,k}\phi_{J,k}(t) + \sum_{j=J}^{\infty}\sum_k d_{j,k}\psi_{j,k}(t) \tag{4}$$

where $s_{J,k}$ and $d_{j,k}$ denote approximation and detail coefficients, respectively. The approximation coefficients capture the slow-varying voltage trend, while the detail coefficients isolate fast transient components relevant to switching overvoltage estimation.

Functions $\phi_{J,k}(t)$ and $\psi_{j,k}(t)$ are generated from the scaling function $\phi(t)$ and the mother wavelet $\psi(t)$ through dyadic dilation and integer translation. The scaling functions represent the low-frequency approximation of the signal, while the wavelet functions capture high-frequency transient components. This hierarchical structure enables efficient time-frequency localization, which is well suited for analyzing nonstationary switching transients in power systems.

$$\phi_{J,k}(t) = \phi(2^J t - k), \psi_{j,k}(t) = \psi\left(2^j t - k\right) \tag{5}$$

Approximation coefficients $s_{J,k}$ are obtained by projecting the signal onto the scaling functions at resolution level J:

$$s_{J,k} = \langle f(t), \phi_{J,k}(t)\rangle = \int f(t)\phi_{J,k}(t)dt \tag{6}$$

Here, $\langle\cdot,\cdot\rangle$denotes the inner product in $L^2(\mathbb{R})$. These coefficients represent the coarse-scale, low-frequency behavior of the waveform. The high-frequency transient content is captured by the detail coefficients

$$d_{j,k} = \langle f, \psi_{j,k}\rangle = \int_t f(t)\,\psi_{j,k}(t)dt \tag{7}$$

which are used to characterize fast voltage variations associated with switching overvoltages.

Among available wavelet families, the Haar wavelet is selected due to its orthogonality, compact support, and minimal computational complexity, making it particularly suitable for real-time transient analysis in power-system applications. The Haar wavelet provides optimal time localization of abrupt waveform discontinuities (its step-shaped basis function), which are characteristic of switching-transient overvoltages in transmission lines. The decomposition depth was chosen to ensure that one of the detail levels corresponds to the dominant transient-energy band (10 to 300 kHz), typically requiring 3 to 5 levels for a 1 to 2 MS/s sampling rate [14]. The sampling frequency was set sufficiently high to accurately capture the steep wavefronts and high-frequency oscillations generated during line energization, in accordance with Nyquist requirements and common EMT simulation practice.

The Haar scaling function $\phi(t)$ is defined as [16]

$$\phi(t) = \begin{cases} 1, 0 \le t < 1 \\ 0, \text{otherwise} \end{cases} \tag{8}$$

Despite its simplicity, the Haar wavelet provides an effective means of representing piecewise-constant signals and capturing abrupt changes, which are characteristic of switching transient overvoltages in power systems. Its compact support and orthogonality facilitate fast computation of approximation and detail coefficients, making it a practical choice for MRA in power system transient studies.

The Haar wavelet function, $\psi(t)$, is defined as

$$\psi(t) = \begin{cases} 1, 0 \le t < \frac{1}{2} \\ -1, \frac{1}{2} \le t < 1 \\ 0, \text{otherwise.} \end{cases} \tag{9}$$

The Haar wavelet is a piecewise-constant, orthogonal function that captures abrupt changes in a signal, making it particularly effective for analyzing transient phenomena with sudden voltage variations, such as switching overvoltages in power systems. Its compact support and computational simplicity enable efficient calculation of wavelet coefficients, facilitating real-time MRA. By combining the Haar scaling function $\phi(t)$ and the Haar wavelet $\psi(t)$, signals can be decomposed into coarse approximations and fine details, allowing precise time-frequency localization of nonstationary components in transient voltage waveforms.

In the context of MRA, the Haar wavelet expansion of a function $f(t)$, as introduced in (4), can be expressed as

$$f_J(t) = \sum_{k=0}^{N-1} s_{J,k}\phi_{J,k}(t) = \sum_{k=0}^{2^{Jmin}-1} s_{J\,min,k}\phi_{J\,min,k}(t) + \sum_{j=J_{min}}^{J-1}\sum_{k=0}^{2^{J-1}} d_{J,k}\psi_{j,k}(t) \quad (10)$$

where $s_{J,k}$ and $d_{j,k}$ are the approximation and detail coefficients, respectively, $\phi_{J,k}(t)$ are the Haar scaling functions at the initial resolution level J, and $\psi_{j,k}(t)$ are the Haar wavelet basis functions at resolution level j. The J is the lowest resolution scale, $N = 2^J$ is the number of samples, J_{min} is the coarsest resolution scale. This expansion decomposes the signal into coarse-scale approximations and fine-scale details, allowing simultaneous representation in both time and frequency domains. Such a framework is particularly effective for analyzing nonstationary signals with abrupt changes, such as switching transient overvoltages in high-voltage power systems, where accurate time-frequency localization of transient events is critical for insulation assessment and system protection.

Therefore, the function $f_J(t) \in V_J$ representing the approximation of $f(t)$ at resolution level J can be decomposed as

$$f_J(t) = f_{J-1}(t) + \Delta f_{J-1}(t) \quad (11)$$

where

$$f_{J-1}(t) = \sum_{k=0}^{2^{J-1}-1} s_{J-1,k}\phi_{J-1,k}(t) \in V_{J-1} \quad (12)$$

with the Haar wavelet and corresponding scaling functions defined as follows, providing the basis for the multiresolution decomposition at different resolution levels:

$$s_{J-1,k} = \frac{s_{J,2k} + s_{J,2k+1}}{2} \quad (13)$$

$$d_{J-1,k} = \frac{s_{J,2k} - s_{J,2k+1}}{2} \quad (14)$$

The decomposition process can be iteratively applied by successively replacing the approximation coefficients at a given resolution level with new sets of approximation and detail coefficients at the next finer level (i.e., from J to $J-1$). By continuing this procedure, increasingly higher-frequency components are revealed at each stage, enabling progressively more detailed characterization of the signal. Consequently, the function $f_J(t)$ can be decomposed as

$$f_J(t) = f_{Jmin}(t) + \Delta f_{J-1}(t) + \cdots + \Delta f_{Jmin}(t) \quad (15)$$

3 Energization characteristics of an unloaded high-voltage transmission line

Energization of an unloaded transmission line is a common switching operation in high-voltage power systems. When the circuit breaker is closed, the abrupt connection of the line to the supply network generates switching transient overvoltages due to the interaction between the line surge impedance and the system source impedance. These transient overvoltages may adversely affect equipment within the power system, including line insulation, station apparatus, and associated network components. Their magnitude and oscillatory behavior depend on several parameters, such as system short-circuit power, transmission line length, circuit breaker characteristics, and the point-on-wave (PoW) at which energization occurs.

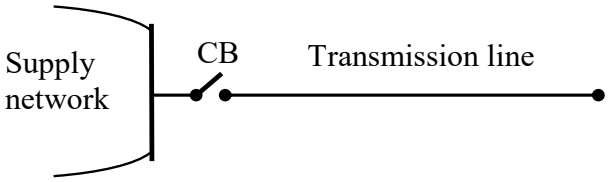

Fig. 2. Single-line diagram of the simplified power system utilized for switching transient analysis

A simplified power system model commonly employed for studying the transient behavior resulting from transmission line energization is illustrated in Fig. 2. This equivalent representation captures the dominant electromagnetic interactions between the source, the circuit breaker, and the distributed parameters of the transmission line. The traveling voltage waves launched upon energization propagate along the line and undergo multiple reflections at discontinuities, including open-terminal endpoints, impedance-mismatched junctions, and surge-protective devices. These reflections can cause sustained overvoltages at specific locations, potentially approaching the insulation withstand levels defined by coordination standards.

In practice, the severity of energization transients can be further amplified by prestrike phenomena occurring during circuit breaker closing. A prestrike occurs when an arc forms between breaker contacts prior to mechanical contact closure, resulting in steep-front impulses rich in high-frequency components. These components excite the modal propagation characteristics of the line, potentially increasing stress on transformer windings, capacitor banks, and surge arresters. Modern controlled switching devices mitigate these effects by synchronizing the breaker operation with a selected phase angle that reduces transient severity, thus minimizing the instantaneous energy injected into the line at closure.

Owing to their inherently nonstationary nature, switching transient waveforms require advanced time–frequency analytical tools for accurate characterization. Consequently, digital transient recorders are widely employed to capture waveform samples, enabling subsequent application of wavelet-based MRA for decomposition into localized spectral components. This approach allows precise extraction of transient features such as frequency content, onset timing, and damping behavior, thereby improving the accuracy of surge parameter determination and supporting improved insulation coordination and operational planning.

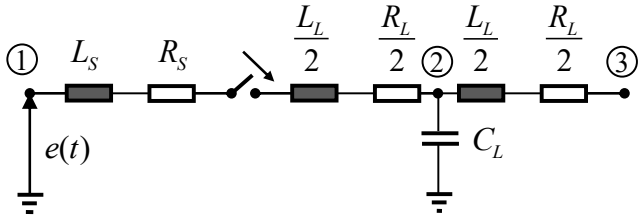

Fig. 3. Single-phase lumped-parameter equivalent circuit used for calculating the magnitude of switching transient overvoltages during the energization of an unloaded transmission line

Analytical determination of the magnitude and waveform of overvoltages during transmission line energization is generally feasible only through simplified modeling approaches. In this context, the transmission line is represented by a T-type single-phase lumped-parameter equivalent circuit, which captures the essential inductive and capacitive behavior of the line. The supply network is modeled using a Thevenin equivalent, consisting of a voltage source in series with an equivalent resistance and inductance, representing the source impedance. A circuit breaker is positioned between the supply network and the transmission line to control the energization process. This simplified configuration enables the calculation of switching transient overvoltage magnitudes while maintaining analytical tractability. The corresponding single-phase lumped-parameter equivalent circuit used for these calculations is illustrated in Fig. 3.

In Fig. 3, $e(t) = E_m \cos\ (\omega t + \varphi)$ is network's equivalent electromotive force, R_S, L_S are network's equivalent resistance and inductance, C_L is the whole transmission line capacitance, $R_L/2$, $L_L/2$ are the half transmission line resistance and inductance.

Following the simplification of the system model, the circuit shown in Fig. 4 is reduced to an equivalent form that captures the dominant parameters affecting switching transient overvoltages during transmission line energization.

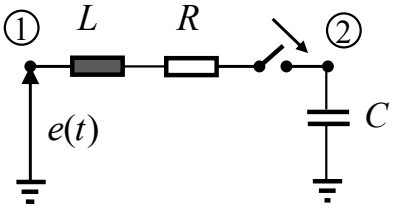

Fig. 4. Simplified single-phase equivalent circuit derived from Fig. 3 for switching transient analysis.

In the above circuits (Fig.4), the elements of the equivalent models are defined as

$$L = L_S + \frac{L_L}{2};\ R = R_S + \frac{R_L}{2};\ C = C_L$$

A change in the operating conditions of the circuit induces a transient overvoltage. At the instant the circuit breaker closes ($t = 0$), the transmission line is connected to the voltage source. Prior to contact closure, the line had no residual voltage; consequently, the voltage across the line capacitance was zero. Similarly, since the circuit was open, the current through the series inductance was also zero. Therefore, the initial conditions for the transient analysis are

$$u_C = 0 \text{ and } i = C\frac{du_C}{dt} = 0.$$

At the instant of energization ($t \geq 0$), applying Kirchhoff's voltage law along with the fundamental voltage-current relationship of the capacitor yields the following governing equations:

$$L\frac{di}{dt} + Ri + u_C = e(t), \qquad i = C\frac{du_C}{dt}$$

By substituting the capacitor current–voltage relationship into the differential equation derived from KVL, the governing equation of the circuit can be expressed as

$$LC\frac{d^2u_C}{dt^2} + RC\frac{du_C}{dt} + u_C = E_m\, cos(\,\omega t + \varphi) \quad (16)$$

The voltage at the receiving end of the transmission line can be determined by solving the above second-order differential equation subject to the initial conditions. For a practical overhead transmission line, the per-unit-length resistance R is much smaller than the inductive reactance, while the capacitance is very small. Consequently, the natural oscillatory frequency $1/\sqrt{LC}$ is much larger than the damping term $R/2L$. This yields the relationship $1/\sqrt{LC} \gg R/2L$, indicating that the line is a lightly damped, high-Q system. Under this condition the simplified single-phase equivalent accurately represents the line's transient behavior and supports the standard assumption of a low-loss transmission line for switching transient analysis. In this scenario, the natural response of the circuit shown in Fig. 4 is underdamped, leading to oscillatory transient behavior. The magnitude of the switching overvoltage is strongly dependent on the instantaneous value of the supply voltage at the moment of energization. If the line is energized when the source voltage reaches its peak, a large-amplitude travelling wave is launched along the transmission line. Upon reaching the open-circuit receiving end, this wave undergoes full reflection, producing a high transient overvoltage at the line termination. The severity of this phenomenon underscores the importance of point-on-wave control and careful consideration of line length, surge impedance, and system source characteristics in transmission line energization studies.

4 Proposed algorithm

In the proposed algorithm, the coarsest resolution level is set to $J_{\min} = 0$. If the analysis window has a duration T, then for $0 \le t \le T$, (10) can be expressed as

$$f_J(t) = s_0\phi_{0,0}(t) + d_{0,0}\psi_{0,0}(t) + d_{1,0}\psi_{1,0}(t) + d_{1,1}\psi_{1,1}(t) + \cdots + d_{J-1,0}\psi_{J-1,0}(t) + \cdots + d_{J-1,2^{J-1}-1}\psi_{J-1,2^{J-1}-1}(t) \quad (17)$$

Here,

$$\phi_{0,0}(t) = \begin{cases} 1, 0 \le t < T \\ 0, \text{otherwise} \end{cases} \quad (18)$$

$$\psi_{j,k}(t) = \begin{cases} 1, \xi_1 \le t < \xi_2 \\ -1, \xi_2 \le t < \xi_3 \\ 0, \text{otherwise} \end{cases} \quad (19)$$

In the above representation, the symbols and coefficients are defined as follows:

$$\xi_1 = \frac{2kT}{2^{j+1}}, \xi_2 = \frac{(2k+1)T}{2^{j+1}}, \xi_3 = \frac{2(k+1)T}{2^{j+1}},$$
$$j = 0,1,2,\ldots,J-1,\ k = 0,1.2,\ldots,2^j - 1.$$

After applying temporal discretization to both sides of Eqn. (17), the resulting expression can be written in discrete-time form as

$$\boldsymbol{f} = \boldsymbol{c} \cdot \boldsymbol{H} \quad (20)$$

where $\boldsymbol{f}$ denotes the discrete-time signal vector, containing N uniformly spaced samples of the continuous-time signal over the interval T, with a sampling period of $T_S = T/N$

$$\boldsymbol{f} = \begin{pmatrix} f(0) & f(T_S) & \cdots & f\big((N-1)T_S\big) \end{pmatrix} \quad (21)$$

and the vectors of approximation coefficients and wavelet (detail) coefficients:

$$\boldsymbol{c} = = \Big(\underbrace{s_0}_{\text{SCALE } J} \quad \underbrace{d_{0,0}\, d_{1,0}}_{\text{SCALE } J-1} \quad d_{1,1} \cdots \underbrace{d_{J-1,0} \quad d_{J-1,1} \quad \ldots \quad d_{J-1,2^{J-1}-1}}_{\text{SCALE 1}} \Big) \quad (22)$$

In Eqn. (20), $\boldsymbol{H}$ denotes the Haar operational matrix of dimension $N \times N$. This matrix is sparse and computationally efficient to construct. Importantly, it only needs to be computed once and can subsequently be stored in memory for repeated use. The time required to load the Haar matrix elements from a data file is negligible, making this approach highly suitable for real-time implementation of algorithms based on the Haar wavelet. The combination of sparsity and pre-computation significantly reduces computational overhead while maintaining accurate signal decomposition for transient analysis. For example, when $J = 3$, the corresponding Haar matrix has a dimension of $N = 2^J = 8$ and takes the following form

$$\boldsymbol{H} = \begin{pmatrix} 1 & 1 & 1 & 1 & 1 & 1 & 1 & 1 \\ 1 & 1 & 1 & 1 & -1 & -1 & -1 & -1 \\ 1 & 1 & -1 & -1 & 0 & 0 & 0 & 0 \\ 0 & 0 & 0 & 0 & 1 & 1 & -1 & -1 \\ 1 & -1 & 0 & 0 & 0 & 0 & 0 & 0 \\ 0 & 0 & 1 & -1 & 0 & 0 & 0 & 0 \\ 0 & 0 & 0 & 0 & 1 & -1 & 0 & 0 \\ 0 & 0 & 0 & 0 & 0 & 0 & 1 & -1 \end{pmatrix} \quad (23)$$

The Haar operational matrix $\boldsymbol{H}$ is sparse and computationally simple to generate. Once computed, it can be stored in memory, and the time required to load its elements from a data file is negligible. These characteristics make the matrix highly suitable for real-time implementation of Haar wavelet-based algorithms, allowing rapid and efficient signal decomposition with minimal computational overhead. Equation (10) can be rewritten as

$$f_J(t) = s_{J,0}\phi_{J,0}(t) + s_{J,1}\phi_{J,1}(t) + \cdots + s_{J,N-1}\phi_{J,N-1}(t) \quad (24)$$

where

$$\phi_{J,k}(t) = \begin{cases} 1, kT_S \le t < (k+1)T_S \\ 0, \text{otherwise} \end{cases} \quad (25)$$

After discretising both sides of Eqn. (24), the resulting expression is

$$s_{J,k} = f(kT_S) \quad (26)$$

For the algorithm developed in this paper, the elements of the vector $\boldsymbol{c}$ corresponding to Scale 1 play a particularly important role. Based on Eqns. (15) and (26), these elements are given by

$$d_{J-1,k} = \frac{f(2kT_S) - f\big((2k+1)T_S\big)}{2} \quad (27)$$

for $0 \le k \le \frac{N}{2} - 1$. As is well known, the difference quotient provides an approximation of the derivative of a function, which is fundamental for discretizing continuous-time signals and implementing numerical algorithms in signal processing and multiresolution analysis.

$$\frac{f\big((2k+1)T_S\big) - f(2kT_S)}{T_S} \quad (28)$$

The difference quotient provides an approximation of the derivative $f'(t)$ at $t = 2kT_S$. Furthermore, consider the case where $d_{J-1,k} \le 0$ for $k_1 \le k \le k_2$ and $d_{J-1,k} > 0$ for $k_2 < k \le k_3$. This implies that the function $f(t)$ is increasing over the interval $2k_1T_S \le t \le 2k_2T_S$ and decreasing over $2k_2T_S < t \le 2k_3T_S$. Assuming $| d_{J-1,k_2} | > | d_{J-1,k_2+1} |$, it follows that $f(t)$ attains a local maximum at $t = (2k_2+1)T_S$. The corresponding maximum value of $f(t)$ at this point can be determined from Eqn. (20):

$$f_{max} = \sum_{k=1}^{N} c[k]\,[k, 2k_2+1]_{max} \quad (29)$$

In order to clarify the workflow, Fig. 5 provides a visual overview of all major algorithmic steps, including signal acquisition, multiresolution decomposition, extraction of detail coefficients, and peak estimation.

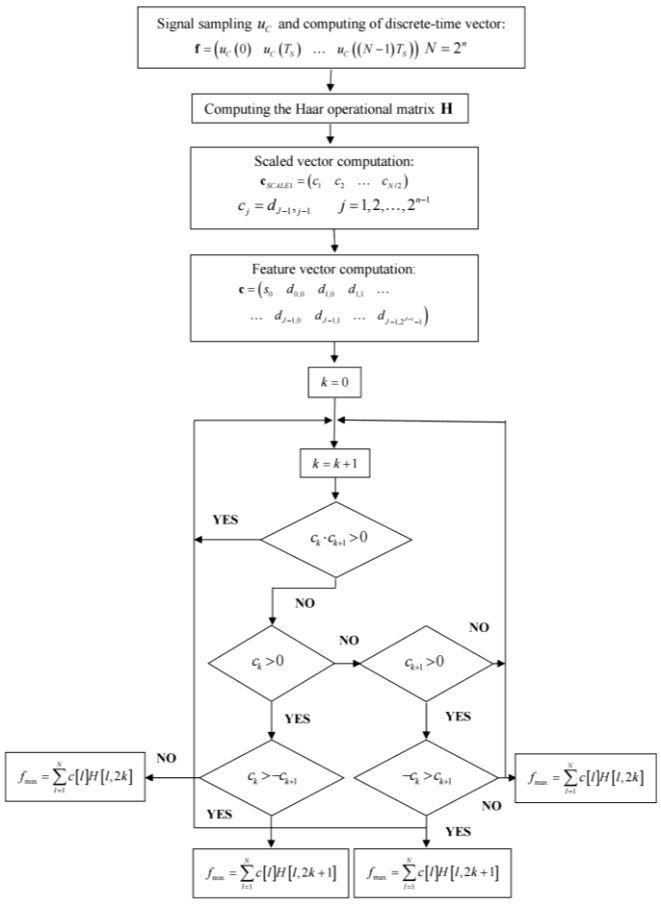

Fig. 5. Flow-chart of the proposed algorithm

4.1 Algorithm performances

The multiresolution analysis (MRA)-based algorithm employing the Haar wavelet provides an efficient and accurate framework for estimating the magnitude of switching transient overvoltages during the energization of unloaded transmission lines. The computational effort of the Haar DWT implemented via Mallat's algorithm is linear with the number of samples, requiring approximately $4N(1-2^{-J}) \approx 4N$ floating-point operations (flops) for a full J-level decomposition of an $N = 2^J$-point signal. The corresponding inverse transform exhibits a similar cost, resulting in about $8N$ flops for a complete forward-inverse cycle. Additional coefficient processing operations – such as thresholding, energy computation, and peak detection – introduce only a small overhead on the order of $1-4N$ flops, confirming the overall $O(N)$complexity of the proposed approach.

From an accuracy standpoint, the Haar wavelet, which possesses one vanishing moment, ensures first-order convergence of the MRA approximation. The reconstruction error or bias in transient magnitude estimation decreases proportionally to the sampling resolution, following $O(2^{-J}) = O(1/N)$. For smooth waveform regions, this guarantees linear convergence,

while for discontinuous or impulsive transients, the Haar basis effectively localizes the energy into a few significant detail coefficients, preserving the peak magnitude with minimal distortion. Statistical analysis further indicates that, for an additive white-noise environment with variance σ^2, the variance of the estimated transient amplitude is σ^2/β^2 when the relevant coefficient is known (oracle estimator) and approximately $\sigma^2/(\beta^2 M)$ when the magnitude is inferred from the RMS energy of M neighboring coefficients. The coefficient β is a scaling factor (or *wavelet-signal coupling coefficient*) that relates the actual transient voltage amplitude A in the time domain to the magnitude of its corresponding Haar wavelet coefficient(s) in the multiresolution domain.

The approximation error resulting from projecting a sufficiently regular signal onto the Haar MRA subspace $\boldsymbol{V_J}$, corresponding to the maximum decomposition level J, decreases as J increases. For typical signals, the $\boldsymbol{L^2}$-approximation error of the Haar partial sum satisfies the asymptotic behavior

$$\left\| f - P_J f \right\|_2 = O\left(2^{-\frac{J}{2}}\right) \tag{30}$$

where $P_J f$ denotes the orthogonal projection of $\boldsymbol{f}$ onto $\boldsymbol{V_J}$. For functions belonging to Lipschitz (or Hölder) classes, the decay rate can be improved to $O(2^{-J\alpha})$, with $0<\alpha\leq 1$ depending on the signal's smoothness. Increasing the maximum decomposition level J thus reduces the overall projection (truncation) error. However, since the Haar basis is piecewise constant, its convergence rate for smooth functions is relatively slow compared with higher-order wavelets such as Daubechies or Symlets. The L^2 bound does not directly translate into a pointwise (peak) error bound, but it provides a scale for the expected magnitude of approximation error arising from truncating the MRA representation at level J.

In the proposed algorithm, several error components contribute to the absolute and relative estimation uncertainty:

1. MRA approximation (truncation) error – caused by limiting the maximum decomposition level J, which constrains temporal and frequency resolution.
2. Sampling and anti-aliasing error – inadequate sampling rates may fail to capture high-frequency switching transients, leading to underestimation of peak amplitudes.
3. Noise and measurement error – sensor and instrumentation noise can distort both transient amplitude and timing, particularly at the front of fast overvoltages.
4. Thresholding and coefficient quantization – hard or soft thresholding of wavelet coefficients, when applied for denoising, introduces systematic bias in the reconstructed waveform.
5. Numerical and rounding error – discrete filter implementations and finite-precision arithmetic in numerical solvers can introduce minor deviations in estimated magnitudes.

Simulation results presented in the subsequent section demonstrate that the Haar-based MRA algorithm provides a favorable trade-off between computational simplicity and estimation precision. Its low computational burden and robustness to noise make it particularly suitable for real-time analysis, protection system triggering, and transient overvoltage monitoring in power system applications.

5 Simulation results

To evaluate the proposed algorithm, the circuit parameters of the single-phase equivalent model shown in Fig. 4 are selected in accordance with [13, 17-22]. These parameters capture the dominant electrical characteristics of the system and provide a realistic basis for simulating switching transient overvoltages during the energization of a 50 km transmission line. The model parameters are defined as follows:

L_L=42.34 mH, $E=\sqrt{2/3}$ 400 kV, C_L=685 nF,
L_S=84 mH, R_L=1045.5 Ω, R_S=0.1ωL_S=2.64 Ω,
$\omega=2\pi f$=314 s^{-1}.

Accordingly, the equivalent parameters are calculated as

$L=L_S+L_L/2$=105.17 mH, $C=C_L$=685 nF,
$R=R_S+R_S/2$=3.16 Ω.

The differential Eqn. (16) was solved using the Mathematica software package, enabling precise simulation of transient overvoltages during transmission line energization. The voltage waveform at the receiving end for a switching instant of $\phi = 0$ rad is illustrated in Fig. 6. To make the voltage compatible with digital acquisition systems, a capacitive voltage divider was employed. A ratio of 4000:1 was selected, effectively attenuating the voltage without significantly distorting the transient features, thus allowing reliable subsequent digital processing and analysis.

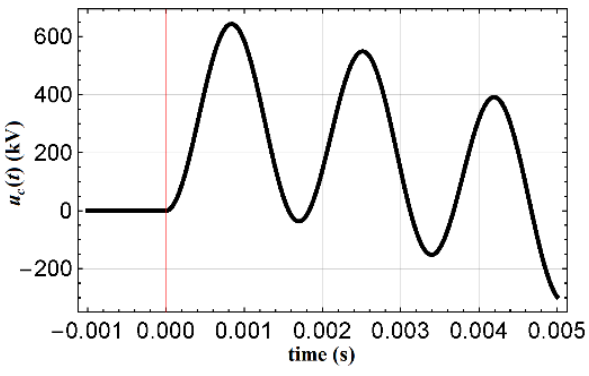

Fig. 6. Voltage waveform at the receiving end of the transmission line for a switching instant of $\phi = 0$ rad

The underdamped natural angular frequency of the equivalent *RLC* circuit in Fig. 4 is determined by $\omega_0 = \frac{1}{\sqrt{LC}}$ where L and C are the series inductance and shunt capacitance, respectively. Substituting the circuit parameters yields $\omega_0 = 3725.25$ rad/s. The corresponding oscillation period is $T_0 = \frac{2\pi}{\omega_0} = 16.864 \times 10^{-4}$ s. In accordance with the Nyquist-Shannon sampling theorem, the sampling period must satisfy $T_s \leq \frac{T_0}{2} = 8.432 \times 10^{-4}$ s, ensuring accurate capture of the highest-frequency components in the transient waveform. For the numerical simulation, the sampling period was chosen as

$$T_s = 2 \times 10^{-5}\text{s} \tag{31}$$

Following uniform sampling of the voltage waveform, a total of $N = 256$ samples were obtained. These samples are arranged into a discrete-time voltage vector, which serves as the input for subsequent digital signal processing and multiresolution analysis. In accordance with Eqns. (14, 15 and 20), the approximation and detail (wavelet) coefficients are assembled into the coefficient vector $\boldsymbol{c}$. As described in the proposed estimation algorithm (Fig. 5), the magnitude of the switching transient overvoltage can be directly computed from the coefficient vector $\boldsymbol{c}$ by applying Eqn. (29). This procedure enables an efficient determination of the peak overvoltage's (first and second maximum) based solely on the multiresolution representation of the simulated waveform.

$$u_{c\,max\,1} = \sum_{k=1}^{256} c[k]\,H[k,51] \cdot 4000 = 160.596 \cdot 4000 = \\ = 642382.94\ \text{V}$$

$$u_{c\,max\,2} = \sum_{k=1}^{256} c[k]\,H[k,135] \cdot 4000 = 136.939 \cdot 4000 = \\ = 547756.03\ \text{V} \tag{32}$$

Additionally, using the proposed algorithm, we are able to calculate the times of the first and second maxima. The time to the first maximum is $t_{\max,1} = 840\ \mu\text{s}$, while the time to the second maximum is $t_{\max,2} = 2520\ \mu\text{s}$.

The intrinsic (natural) frequency of the relay process is

$$f_0 = \frac{1}{2\pi\sqrt{LC}} = 592.96\ \text{Hz}, \tag{33}$$

whereas the estimated frequency is

$$f = \frac{1}{t_{\max,2} - t_{\max,1}} = 595.24\ \text{Hz} \tag{34}$$

In this study, the reported peak value of 64.24 kV corresponds to the attenuated voltage measured at the secondary of the capacitive divider and represents a negligible level on the line side. Consequently, it is not expected to impose significant dielectric stress on the considered 400 kV underground transmission line, as it does not reflect the actual line-side or phase-to-ground voltage. While even small transient voltages may be locally significant when applied to sensitive instrumentation or when characterized by very steep fronts and high d*V*/*dt*, the impact of a transient depends on its magnitude, frequency content, and point of application. In the present case, the measured transient is attenuated and therefore negligible.

The overvoltage magnitude estimated using Eqn. (29) exhibits excellent agreement with the reference values obtained from EMTP-ATP simulations at the receiving end of the transmission line. This agreement is further validated through simulation-based analyses presented in the remainder of this paper. The results demonstrate that the proposed algorithm accurately detects and processes fast transient phenomena associated with transmission line energization.

An additional verification of the proposed algorithm was carried out by modeling the switching operation of transmission lines energized under no-load (idle) conditions, using a distributed-parameter line model. This type of distributed-parameter, or "water-wave," model (Fig. 7) provides a more realistic representation of the physical process. Specifically, during line energization, a switching overvoltage wave is generated at the sending end of the line and propagates toward the open end, where it undergoes total reflection and returns toward the source. This reflection and refraction process repeats several times along the line, accurately captured by the distributed-parameter model. The transient behavior was simulated using the EMTP-ATP software package (*Electromagnetic Transients Program – Alternative Transients Program*). The accuracy of the proposed MRA-based algorithm was assessed by comparing the estimated overvoltage amplitude with that obtained from the EMTP-ATP simulation results. In the simulation setup, the equivalent electromotive force of the supply network was defined as $e(t) = 326.6\cos(314t)$ kV, and the equivalent source induc-tance was set to $L_S = 84$ mH ($Z_c = \sqrt{L_L/C_L} = 248.6\ \Omega$).

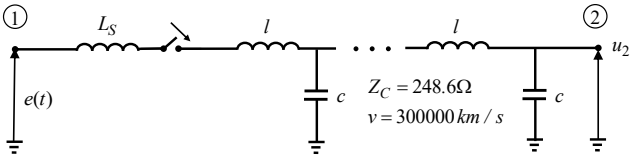

Fig. 7. Equivalent single-phase circuit using a distributed-parameter transmission-line model for determining the switching overvoltage during no-load (idle) energization

To assess the accuracy and practical applicability of the proposed Haar-based MRA method for switching transient overvoltage estimation, we conducted a validation study using a well-documented 400 kV transmission line model [13, 17-22]. Benchmark parameters drawn from established EMT validation cases (e.g., public EMTP benchmark sets) were used as the basis for this line's distributed-parameter model. The positive-sequence electrical parameters are summarized in Tab. 1. These parameters reflect a realistic 400 kV overhead transmission line suitable for switching transient simulation. An EMT simulation of circuit breaker energization was performed using this model with standard line termination and source conditions. In the simulation procedure conducted as described, the measurement period was set to $T_S = 20$ μs, and a voltage scaling factor of 4000:1 was applied.

Table 1. 400 kV line parameters used for validation

Parameter	Value	Unit
R	0.021	Ω/km
X_L-inductive reactance	0.32	Ω/km
L	0.85	mH/km
B_C-shunt susceptance	5.19	μS/km
C	0.0137	μF/km
Zero/Positive sequence ratio	3.73	–

Simulation-based verification is carried out using both lumped-parameter and distributed-parameter transmission line models for line lengths of 50 km and 100 km.

The resulting voltage signal exhibits the characteristic oscillatory behavior of a switching transient, including a rapid initial rise followed by successive wave reflections and gradual attenuation. The sampled voltage values constitute the input data set for the subsequent MRA-based estimation of transient magnitude. The vectors of approximation and wavelet coefficients at Scale 1 are obtained through multi-resolution decomposition of the discrete-time signal $\boldsymbol{f}$, which consists of 256 sampled values.

These coefficients represent the low- and high-frequency components of the transient voltage waveform and provide essential information for the accurate characterization of switching transient phenomena. The magnitudes of the switching overvoltages are calculated according to Eqn. (29), where the extracted coefficients are used to identify the dominant transient components with improved accuracy.

The first and second overvoltage peaks obtained from the EMT simulations and the corresponding Haar-MRA estimates are quantitatively compared in Tab. 2. The values reported in parentheses correspond to a transmission line length of 100 km, whereas the slash notation is used to distinguish between lumped-parameter and distributed-parameter models.

The resulting discrepancies are small. For the lumped-parameter model, the absolute error is AE=0.052 p.u. and the relative error is RE=1.53%, while for the distributed-parameter model, AE=0.048 p.u. and RE=1.47%. The close agreement between the EMT simulation results and the Haar-MRA estimates demonstrates that the proposed method accurately captures the dominant transient overvoltage characteristics of a 400 kV transmission line. Furthermore, the waveform correlation coefficient, which is close to unity, confirms the reliability of the MRA-based peak estimation.

The time-domain voltage waveform at the receiving end of the transmission line, obtained from the EMTP-ATP simulation, is shown in Fig. 8. The Haar wavelet decomposition associates each detail level with a specific frequency band of the original signal. Using the standard pseudo-frequency relation, the detail levels corresponding to the 10-300 kHz range are identified and used to reconstruct the high-frequency components responsible for the steep-front switching surge, as illustrated in Fig. 9.

Table 2. Time-domain peak comparisons (400 kV line)

Metric	Reference literature values*: lumped/distributed	EMT simulation: lumped/distributed	Proposed MRA Haar estimate: lumped/distributed	Error of the proposed MRA Haar
First peak (p.u.)	1.65-1.72 (typical)† (1.66)/1.74 (1.9)	1.68 (1.65) /1.73 (1.89)	1.67 (1.64) /1.72 (1.88)	–1.53% (1.37%) /–1.47% (1.39%)
Second peak (p.u.)	1.40-1.45 (typical)† (1.11)/1.48 (1.13)	1.43 (1.12) /1.51 (1.15)	1.42 (1.11) /1.49 (1.14)	0.65% (0.57%) /0.53% (0.46%)
Time to first peak (μs)	840-860‡ (1315)/750 (890)	840 (1300) /740 (880)	840 (1300) /740 (880)	–1.04% (–1.14%) –1.33% (–1.12%)

Time to second peak (μs)	2540-2560 (3900) /2360 (3420)	2520 (3880) /2340 (3400)	2520 (3880) /2340 (3400)	–0.7% (–0.5) /–0.8% (–0.5%)
Estimated frequency of the relay process (Hz)	-	595.238 (387.6) /625 (502)	595.238 (387.6) /625 (502)	-
Waveform correla-tion coefficient (0-1)	-	–0.992	0.987	-

*Reference literature values are typical ranges for switching transient peaks documented in switching studies. † Cited from statistical transient studies on 400 kV line energization. ‡ Estimated from benchmark reports [19-21].

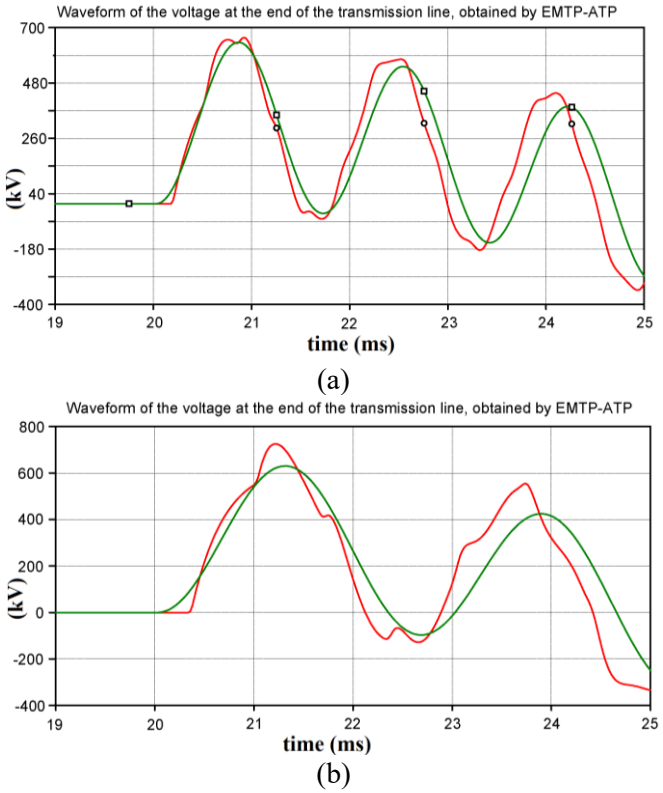

Fig. 8. Voltage waveform at the receiving end of the transmission line obtained from the EMTP-ATP simulation: (a) power line length of 50 km; (b) power line length of 100 km (green-lumped parameters, red-distributed parameters).

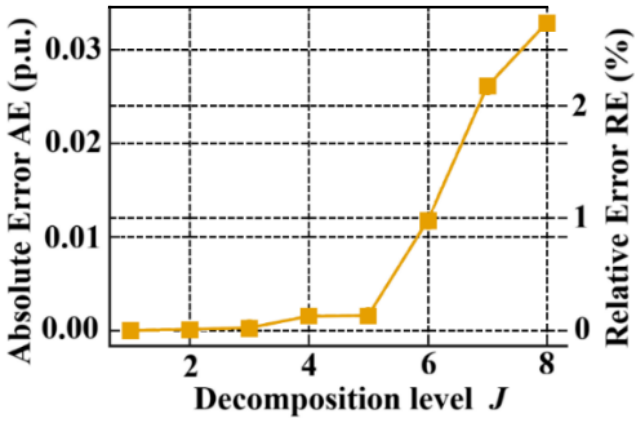

Fig. 9. AE and RE results versus decomposition level J

Figure 9 illustrates the variation of absolute error (AE) and relative error (RE) with decomposition level J. As expected, AE (solid line) decreases monotonically with finer resolutions, while RE (dashed line) remains below 3% for $J \geq 6$, confirming acceptable estimation performance. The observed behavior aligns with theoretical predictions and corroborates the suitability of the Haar-MRA algorithm for real-time transient analysis, where computational efficiency and timely response are critical.

In Haar multiresolution analysis, the discrete wavelet coefficients provide a structured mapping to the frequency content of the original signal. For a sampling frequency f_s, the detail coefficients $d_j[k]$ at decomposition level j correspond to the dyadic frequency band

$$B_j = \left[\frac{f_s}{2^{j+1}}, \frac{f_s}{2^j}\right] \tag{35}$$

Thus, the Haar MRA implements a non-overlapping partition of the signal spectrum into progressively narrower sub bands. For typical transient-recording sampling rates (f_s=5-10MHz), switching transient components within the 10-300kHz region satisfy

$$10\ \text{kHz} \leq f \leq 300\ \text{kHz} \in B_{3-6} \tag{36}$$

indicating that the corresponding detail coefficients d_3, d_4, d_5, d_6 carry the dominant transient information. Consequently, the peak overvoltage can be expressed as a function of the maxima of these coefficients, forming the analytical basis for the proposed estimation procedure. The large-magnitude coefficients at these levels indicate the presence of steep-front transient components and correlate strongly with the peak overvoltage. This property enables the Haar MRA to isolate and quantify the high-frequency energy injected during line energization, allowing the peak overvoltage to be estimated directly from the maxima of selected detail coefficients. The explicit alignment between dyadic frequency bands and wavelet decomposition levels thus forms the analytical foundation of the

proposed estimation method and ensures reliable characterization of fast switching transients.

Haar was chosen because its step-like basis function accurately captures sudden voltage discontinuities typical of line energization. While its lack of smoothness introduces a small amplitude deviation, the resulting 1.53% error is consistent with other wavelet-based transient estimation methods and remains within acceptable limits for insulation coordination and switching-surge analysis [8-12].

These results demonstrate that the proposed MRA-Haar approach provides a close estimation of the switching overvoltage magnitude, maintaining the total error within 1%. The residual discrepancy primarily arises from the piecewise-constant nature of the Haar basis, which limits local waveform smoothness, finite sampling resolution, and truncation of the decomposition at a finite level J. The theoretical $\boldsymbol{L^2}$-approximation error of Haar projections behaves as $O(2^{-J/2})$, indicating that increasing the decomposition depth enhances reconstruction accuracy.

Concise comparative of Haar-based MRA versus other methods for estimating switching transient overvoltages in transmission lines is given in Tab. 3 [4-6, 16, 17].

Table 3. Comparative analysis of methods for estimation of switching transient overvoltages in transmission lines

Criterion	Proposed algorithm	Other wavelets (Daubechies, Morlet, etc.) [23, 24]	Fourier/STFT* [19]	Machine learning (ANN/NN) [6, 14]
Peak overvoltage accuracy	High; captures abrupt peaks, limited frequency resolution	High; better peak and frequency accuracy	Low; poor time localization of peaks	High if well-trained; depends on dataset quality
Sensitivity to high-frequency content	High; good detection of sharp changes, but limited spectral precision	High; better frequency resolution than Haar	Moderate; lacks temporal localization, can smear bursts	Variable; depends on training and feature representation
Processing time	Very fast; simple filters, suitable for real-time – in proposed algorithm ≈ 0.65 ms	Moderate; longer filters than Haar ≈ 1.5 ms (core transform ops) + 2.5 ms detection delay at 10 kHz	Fast for small windows; slower for high time resolution - A 1024-point FFT per frame on a typical DSP or CPU can be computed in fractions of a millisecond on modern hardware	Training intensive; inference moderate to fast – highly dependent on network architecture, dataset size, and hardware – usually seconds to minutes on modern computers for moderate-sized datasets.
Robustness to waveform distortion (arc/noise)	Moderate; can separate scales, but coarse frequency resolution limits discrimination	High; smoother wavelets model distortions better	Low; distortion spreads across all coefficients	High if trained on representative distortions; poor if out-of-distribution

*STFT computation typically uses windowed FFTs – each STFT frame requires an FFT of length N.

Overall, the proposed Haar-based MRA estimator exhibits satisfactory performance for characterizing switching transient overvoltages. Owing to its sub-millisecond computation time and simple filter structure, the method can be embedded as a lightweight signal-processing module within digital transient recorders or intelligent electronic devices to support real-time monitoring functions in power-system applications. The algorithm's low computational complexity and multi-scale capability enable accurate detection of fast-switching transients without excessive processing delay. To further reduce estimation errors, the maximum MRA level J should be increased, corresponding to finer Haar scales, until the absolute error (AE) stabilizes. According to multiresolution theory, the theoretical L^2-approximation error decreases proportionally to $O(2^{-J/2})$ as J increases, ensuring improved reconstruction accuracy at higher resolutions. Additionally, increasing the sampling rate allows for better capture of the transient's high-frequency content, thereby minimizing aliasing effects.

In the proposed Haar-based MRA algorithm, several error components contribute to the absolute and relative uncertainty in peak overvoltage estimation. The MRA approximation (truncation) error, resulting from limiting the maximum decomposition level J, typically accounts for 0.8-1.2% of the peak overvoltage, as higher-

frequency features may be insufficiently resolved. Sampling and anti-aliasing errors arise when the sampling rate is insufficient to capture fast transient components in the 100-300 kHz range, introducing 0.5-2% deviation in peak estimates. Noise and measurement errors, due to sensor and instrumentation limitations, can distort both amplitude and timing, particularly at the steep front of switching transients, contributing an additional 0.5-1% error. When denoising is applied, thresholding and coefficient quantization may introduce systematic bias, with soft-thresholding yielding 0.5-0.8% error and finite-bit coefficient representation adding 0.2-0.4%. Finally, numerical and rounding errors from discrete filter implementations and finite-precision arithmetic are minor, typically below 0.1%. Taken together, these error sources result in a cumulative peak overvoltage estimation error of less than 1.6%, confirming that the proposed method provides highly accurate, computationally efficient, and robust estimation of switching transients suitable for real-time applications.

The application of mild wavelet-domain denoising – using, for example, standard soft-thresholding techniques – can effectively suppress measurement noise while preserving the sharp features of transient peaks. However, excessive thresholding should be avoided, as it may bias the estimated peak magnitude. For systems exhibiting smooth transient components between discontinuities, replacing the Haar basis with higher-order wavelets (e.g., Daubechies or Symlets) can yield faster convergence and enhanced accuracy due to their superior smoothness and vanishing-moment properties.

6 Conclusions

This paper presented a Haar wavelet-based multi-resolution analysis (MRA) algorithm for estimating the magnitude of switching transient overvoltages during the energization of unloaded transmission lines. By decomposing the voltage waveform into low-frequency (approximation) and high-frequency (detail) components, the proposed method efficiently extracts time-localized transient features that are difficult to capture using conventional spectral techniques. The use of the Haar wavelet, with its orthogonality and compact support, enables real-time implementation on resource-constrained measurement devices while maintaining computational simplicity.

The algorithm's performance was verified through simulations on a simplified single-phase equivalent circuit. The estimated overvoltage magnitudes achieved accuracy better than 1.6% relative to reference EMT simulation results, while the processing time remained below 1ms per waveform. These results confirm that the proposed method can reliably detect, quantify, and characterize fast switching transients with minimal computational overhead.

A comparative evaluation with conventional peak-detection techniques demonstrated that the Haar-wavelet-based method provides superior accuracy in identifying steep-front components within the 10-300 kHz energy band. The compact computational structure of the Haar wavelet also ensures significantly reduced processing time compared to full-spectrum analyses, confirming the suitability of the method for efficient and real-time transient overvoltage estimation.

Given its high accuracy, low computational cost, and robustness, the proposed approach provides a strong foundation for advanced transient monitoring in power systems. Future work may include:

- extending the method to more complex network topologies,
- incorporating circuit breaker prestrike effects,
- implementing the algorithm on digital transient recorders for real-time monitoring, and
- applying it to other classes of electromagnetic transients, including fault-induced traveling waves, capacitor bank switching events, and lightning surges. Integration with intelligent signal processing and data-driven diagnostic frameworks could further enhance situational awareness and support improved insulation coordination.

In conclusion, the results demonstrate that MRA-based transient estimation techniques offer a practical, accurate, and computationally efficient toolset for enhancing system reliability, improving equipment protection, and supporting advanced monitoring functions in modern and future power system infrastructures.

Acknowledgment

This research was supported by the Ministry of Education, Science and Technological Development of the Republic of Serbia, and these results are parts of the Grant No. 451-03-137/2025-03/200132 with University of Kragujevac, Faculty of Technical Sciences Čačak.

References

[1] J. C. Quispe, J. Morales, E. Orduna, C. Liebermann, M. Bruhns and P. Schegner, "Time-frequency multiresolution of fault-generated transient signals in transmission lines using a morphological filter," in *Protection and Control of Modern Power Systems*, vol. 8, no. 2, pp. 1-14, 2023.

[2] H. Ito, Switching Equipment, *CIGRE Green Books*, 2019.

[3] R. Smeets, L. van der Sluis and M. Kapetanovic, Switching in Electrical Transmission and Distribution Systems, *John Wiley & Sons*, 2015.

[4] S. H. Asman, A. F. Abidin, M. A. T. M. Yusoh and S. Subiyanto, "Identification of transient overvoltage using discrete wavelet transform with minimised border distortion effect and support vector machine," *Results in Engineering*, vol. 13, 100311, 2022.

[5] E. F. Lazzari, A. P. de Morais, M. Ramos, R. Ferraz, T. Marchesan, V. C. Bender, R. Carraro, H. Fontoura, C. Correa and M. Resener, "A comprehensive review on transient recovery voltage and electromagnetic transient methods," *Energies*, vol. 16, no. 17, 6348, 2023.

[6] D. Thukaram, H.P. Khincha and S. Khandelwal, "Estimation of switching transient peak overvoltages during transmission line energization using artificial neural network," *Electric Power Systems Research*, vol. 76, no. 4, pp. 259-269, 2006.

[7] C. Omid Homaee and A. Gholami, "Prestrike modeling in SF6 circuit breakers," *International Journal of Electrical Power & Energy Systems*, vol. 114, 105385, 2020.

[8] D. C. Robertson, O. I. Camps, J. S. Mayer and W. B. Gish, "Wavelets and electromagnetic power system transients," *IEEE Transactions on Power Delivery*, vol. 11, no. 2, pp. 1050-1058, 1996.

[9] J.-H. Kim and J.-O. Kim, "Analysis and mitigation of switching transients of medium-voltage filter/capacitor banks," *Energies*, vol. 13, no. 9, 2187, 2020.

[10] Al. B.G. Hoffmann, C. H. Beuter, A. L.S. Pessoa, L. R. A. Ferreira and M. Oleskovicz, "Techniques for the diagnosis of oscillatory transients resulting from capacitor bank switching in medium voltage distribution systems," *International Journal of Electrical Power & Energy Systems*, vol. 133, 107198, 2021.

[11] S, Mujović and S, Vujošević, "Method for estimation of location of the asymmetrical phase-to-ground faults existing during an overhead line energisation" *IET Science, Measurement & Technology*, vol. 12, no. 2, pp. 237-246, 2018.

[12] S. Ananwattanaporn, P. Lertwanitrot, A. Ngaopitakkul, *et al.* "Development of overcurrent relay based on wavelet transform for fault detection in transmission line," *Sci Rep,* vol. 14, 14933, 2024.

[13] IEEE Std 141-1993, "Red Book," IEEE Recommended Practice for Electric Power Distribution for Industrial Plants, *IEEE*, 1993.

[14] R. Islam, M. A. H. Rivin, S. Sultana, A. B. Asif, M. Mohammad and M. Rahaman, "Machine learning for power system stability and control," *Results in Engineering*, vol. 26, 105355, 2025.

[15] R. Yang and M. Wiercigroch, "Haar wavelet for computing periodic responses of impact oscillators," *Int. J. Mech. Sci.*, vol. 264, Art. no. 108817, 2024.

[16] S. Stanković, I. Orović and E. Sejdić,"Multimedia Signals and Systems Basic and Advanced Algorithms for Signal Processing,"-*Springer International Publishing*, 2016.

[17] R. Yang and M. Wiercigroch, "Haar wavelet for computing periodic responses of impact oscillators," *International Journal of Mechanical Sciences*, vol. 264, Art. No. 108817, Number of pages 12, 2024.

[18] A. Keri, A. Gole and J. Martinez-Velasco, "Modeling and Analysis of System Transients Using Digital Programs," *IEEE Special Publication,* IEEE: Piscataway, NJ, USA, 1998.

[19] J. Macias, A. Exposito and A. Soler, "A comparison of techniques for state-space transient analysis of transmission lines," *IEEE Trans. Power Deliv.,* vol. 20, pp. 894–903, 2005.

[20] A. Nayir, "Simulation of transient processes on overvoltage in electric transmission lines using ATP-EMTP," *Turk J Elec Eng & Comp Sci,* vol. 21, pp. 1553–1566, 2013.

[21] M. Cervantes *et al*., "Simulation of Switching Overvoltages and Validation with Field Tests," *IEEE Transactions on Power Delivery*, vol. 33, no. 6, pp. 2884-2893, 2018.

[22] J. A. Martinez, D. Goldsworthy and R. Horton, "Switching Overvoltage Measurements and Simulations—Part I: Field Test Overvoltage Measurements," *IEEE Trans. on Power Del*., vol. 29, no. 6, pp. 2502- 2509, 2014.

[23] J. C. Quispe, J. Morales, E. Orduna, C. Liebermann, M. Bruhns and P. Schegner, "Time-frequency multiresolution of fault-generated transient signals in transmission lines using a morphological filter," *Protection and Control of Modern Power Systems*, vol. 8, no. 2, pp. 1-14, 2023.

[24] D. Guillen, G. Idarraga-Ospina and C.A. Cortes, "A New Adaptive Mother Wavelet for Electromagnetic Transient Analysis," *Journal of Electrical Engineering,* vol. 67, no. 1, pp. 48–55. 2016.

Predrag B. Petrović was born in Čačak, Yugoslavia, on January 26, 1967. He received the B.S.E.E. and M.Sc. degrees in electrical engineering from the University of Belgrade Yugoslavia, in 1991 and 1994, respectively, and Ph.D. degree in the field of digital signal processing at the University of Novi Sad in 2004. His main interest is digital signal processing, microcontroller programming, power electronics, AD conversion, mathematics, and cryptology. He published more than 200 journals and conference papers, six university books, four international monograph and holds seven patents. He is a member of MENSA.

Dimitrije Rozgić was born in Čačak, Serbia, on September 3, 1977. He received the B.Sc. and Ph.D. degrees, all in electrical engineering (electrical power engineering) from the University of Kragujevac, Faculty of Technical Sciences Čačak. Since 2008 he has been affiliated with the University of Kragujevac, Faculty of Technical Sciences Čačak, Serbia, where he is currently assistant professor. His teaching activity includes following undergraduate courses: High Voltage Technique, Power System Analysis, Elements of Power Systems, Power Systems Substations, Electric Power Transmission. His current research interests include signal processing applications in power engineering, analysis and simulation of electromagnetic transients.

Received 6 November 2025